HHS Public Access

Author manuscript

Hepatol Res. Author manuscript; available in PMC 2024 March 01.

Published in final edited form as:

Hepatol Res. 2023 March ; 53(3): 208–218. doi:10.1111/hepr.13858.

Early diagnosis of hepatic inflammation in Japanese nonalcoholic fatty liver disease patients using 3D MR elastography

Yasuyuki Komiyama[1], **Utaroh Motosugi**[2], **Shinya Maekawa**[1], **Leona Osawa**[1], **Natsuko Nakakuki**[1], **Hitomi Takada**[1], **Masaru Muraoka**[1], **Yuichiro Suzuki**[1], **Mitsuaki Sato**[1], **Shinichi Takano**[1], **Mitsuharu Fukasawa**[1], **Tatsuya Yamaguchi**[1], **Hiroshi Onishi**[2], **Meng Yin**[3], **Nobuyuki Enomoto**[1]

[1]First Department of Internal Medicine, Faculty of Medicine, University of Yamanashi, Chuo, Yamanashi, Japan

[2]Department or Radiology, Faculty of Medicine, University of Yamanashi, Chuo, Yamanashi, Japan

[3]Department of Radiology, Mayo Clinic, Rochester, Minnesota, USA

Abstract

Background: The damping ratio (DR) and the loss modulus (G″) obtained by 3D MR elastography complex modulus analysis has been reported recently to reflect early intrahepatic inflammation, and is expected to be a noninvasive biomarker of inflammation in nonalcoholic fatty liver disease (NAFLD). However, the role of the DR and the G″ in Japanese NAFLD patients remains unclear.

Methods: We enrolled 39 Japanese patients with NAFLD who underwent liver biopsy and 3D MR elastography within 1 month and analyzed the association between DR, G″, and histological activity.

Results: Regarding DR, no evident correlation was observed between the DR and histological activity ($p = 0.14$) when patients with all fibrosis stages were included. However, when patients were restricted up to stage F2 fibrosis, the association of the DR and inflammation became significant, the DR increasing with the degree of activity ($p = 0.02$). Among the constituents of

Correspondence: Shinya Maekawa, First Department of Internal Medicine, Faculty of Medicine, University of Yamanashi, 1110, Shimokato, Chuo, Yamanashi 409-3898, Japan. maekawa@yamanashi.ac.jp.

SUPPORTING INFORMATION

Additional supporting information can be found online in the Supporting Information section at the end of this article.

CONFLICTS OF INTEREST

The Mayo Clinic and Meng Yin have intellectual property rights and a financial interest in magnetic resonance elastography technology. Other authors declare no Conflict of Interests for this article.

ETHICS STATEMENTS

Approval of the research protocol: The study protocol was approved by the Human Ethics Review Committee of the University of Yamanashi, and conformed to the ethical guidelines of the Declaration of Helsinki.
Informed Consent: Written informed consent was obtained from all patients.
Registration no. of the study: 1326.
Animal Studies: N/A.
Research involving recombinant DNA: N/A.

fibrosis activity, ballooning correlated with the DR ($p < 0.01$) while lobular inflammation did not. Regarding G″, it was correlated with histological activity ($p < 0.01$), ballooning ($p < 0.01$), and lobular inflammation ($p < 0.01$) in patients with all fibrosis stages and in patients up to F2 fibrosis ($p = 0.03$ for activity and $p = 0.04$ for ballooning). The best cutoff value of DR for hepatitis activity in patients within the F2 stage was 0.094 (area under the receiver operating characteristic curve 0.775, 95% CI: 0.529–1.000) and G″ was 0.402 (area under the receiver operating characteristic curve 0.825, 95% CI: 0.628–1.000).

Conclusions: The DR and G″ reflected the histological activity in Japanese patients with NAFLD during the early stage, indicating these values for noninvasive diagnosis of inflammation in Japanese patients with NAFLD.

Keywords

3D MRE; damping ratio; intrahepatic inflammation; loss modulus; NAFLD; NASH

BACKGROUND

In recent years, nonalcoholic fatty liver disease (NAFLD) has become the most common chronic liver disease worldwide, accompanying the increase in lifestyle-related diseases such as obesity and diabetes. In contrast to the decrease of viral hepatitis following advances in antiviral therapy, it is estimated that 20%–30% of adults have NAFLD, worldwide[1] and in Japan.[2,3] Though the prevalence of nonalcoholic steatohepatitis (NASH), a more progressive condition, and its time-dependent changes are not understood precisely in patients with NAFLD, NASH was thought to be becoming more prevalent as the number of patients with NAFLD increases.[4] It is also thought that the number of patients with cirrhosis and hepatocellular carcinoma (HCC) is growing with the increase in NASH.[1,5–8]

In patients with NAFLD, the diagnosis of NASH is clinically important and has been made by liver biopsy; histological information regarding fibrosis, fat accumulation and inflammation, including lobular inflammation and ballooning, has been essential and is indispensable.[1,9] However, liver biopsy is a rather invasive procedure and it is difficult to perform liver biopsies on a large number of patients with NAFLD and, therefore, a noninvasive and simple alternative is required. Several noninvasive methods have been developed for the assessment of liver histology, such as the serum markers M2BPGi, Fibrosis-4 (FIB-4) index, and APRI,[10] as well as medical devices such as Fibroscan and MR elastography (MRE).[11–14] However, most of these serum markers and medical devices focus on the quantitative evaluation of liver fibrosis or fat deposition, but not on hepatic inflammation. Only recently, it was reported that the damping ratio (DR) and the loss modulus (G″), an index of liver viscosity obtained during the three-dimensional (3D) MRE complex modulus analysis, might reflect early inflammation in chronic liver diseases.[15–24] First, this was shown in animal models, including mice with NAFLD, and later it was also reported in human patients with NAFLD. On the other hand, those studies were from the United States and Europe, and the data were obtained primarily from White patients; it remains to be determined whether the findings extend to other ethnic groups.[15–19,21,23,24]

The clinical manifestations and the course of NAFLD may vary among different ethnic groups. For example, Asians have a significant predisposition to metabolic syndrome and NASH, despite having a lower body mass index and lower rates of obesity than other ethnic groups.[25] Although such differences may be caused by multiple genetic and environmental factors and the detailed reasons are not clear, it is possible that the applicability of the DR and the G″ might vary among different ethnic groups.[26–28]

Based on this, we focused our study on the role of the DR and the G″ obtained by 3D MRE in the diagnosis of inflammation in Japanese patients with NAFLD.

PATIENTS AND METHODS

Study population

Between June 2017 and September 2020, 220 patients with a diagnosis of fatty liver (MRI-proton density fat fraction [PDFF] ≥5%) underwent 3D-MRE at the University of Yamanashi Hospital. In 80 of the 220 patients, histological evaluation was performed using liver tissue obtained via liver biopsy or surgical hepatic resection for HCC within 1 month of the 3D-MRE. From these 80 patients, those with a clear history of alcohol consumption (n = 17, defined as drinking more than 30 g/day of ethanol for men and 20 g/day for women) and liver diseases other than NAFLD (viral hepatitis [n = 23] and autoimmune hepatitis [n = 1]) were excluded and, finally, 39 were enrolled to analyze the association between liver histology and MRE parameters (Figure 1). We investigated the relationship between the histological findings of the liver and the parameters related to hepatic viscosity and elasticity obtained through 3D-MRE analysis in all patients and, separately, in those without advanced fibrosis (patients with F2 or lower stages of fibrosis in the Brunt classification, or patients with MRE shear stress values of <3.62 kPa, because that value has been reported to be equivalent to F2 or lower stages of fibrosis).[29]

Histologic evaluation

Thirty-two of the 39 patients had liver tissue collected with a 16G semiautomated biopsy needle (BARD, MONOPTY) under echo guidance; and two samples, at least 10 mm long, were collected. Seven patients were evaluated for background liver histology based on tissue collected during surgery for HCC. All samples were stained with hematoxylin–eosin and Masson's trichrome and evaluated by an experienced pathologist. Liver fibrosis was rated on a 5-point scale from 0 to 4 by Brunt staging. Steatosis (scale: S0–3), lobular inflammation (scale: Lob0–3), and ballooning (scale: Ba0–2) were scored by the NASH Clinical Research Network system and their unweighted sum formed the NAFLD activity score (scale: A0–8). These classifications were evaluated before the statistical analysis.

Imaging parameters of echo-planar imaging MR elastography

All imaging studies were performed using a 3.0-T MRI scanner (Discovery MR750; GE Healthcare) with a 32-channel phased-array coil. After fasting for at least 6 h, participants were investigated in the supine position, and a circumferential elastic band used to secure the passive driver against the upper abdomen. The MRE imaging sequence was spin-echo echo-planar imaging with a 60-Hz frequency of the pneumatic driver. Three alternation

orthogonal motion-encoding gradients were used, with a 96 × 96 in-plane acquisition matrix, 500 ms repetition time, 50 ms echo time, 5 mm section thickness, seven slices, 40 × 40 cm field of view, parallel imaging factor of 2, and 4 phase offsets. Direct inversion was achieved using Helmholtz equation to calculate the complex shear modulus (G*). Four mechanical parameters were derived from G*, including shear stress (|G*|), storage modulus (G′), loss modulus (G″), and DR (G″/2G′). Maps of the shear stress, storage modulus, and loss modulus, all in kilopascals, were read by MRE Lab software (Mayo Clinic). G′ reflects liver elasticity and G″ reflects liver viscosity.

Image analysis

The mechanical parameters of the imaging data were measured by Dr. Y.K. (with 3 years' experience in MRE) without accessing the clinical and biochemical data. The volume region of interest (ROI) was drawn geographically on the liver scan and routine MRI scans were referenced for manual adjustment of adjacent anatomical landmarks. The mean shear stiffness of the liver was calculated using manually designated ROIs. The ROI was drawn manually, encompassing the largest possible area of liver parenchyma where coherent shear waves were visible, while excluding major blood vessels seen on the MRE magnitude image. To avoid areas of incoherent waves, the area immediately below the passive driver was avoided, keeping about 1 cm inside the liver border and including a minimum of 500 pixels per slice. ROIs were set up in center three slices by discarding edge twos, and the overall average stiffness of the liver was reported by recording the average stiffness value for each ROI and calculating the average value, weighted by the ROI size. To assess the reproducibility of 3D MRE, parameters were evaluated twice with an interval of at least 4 weeks.

Statistical analysis

Continuous variables are presented as the median and IQR, categorical variables as numbers and frequencies, and the Kruskal–Wallis test was used to compare histological parameters with their corresponding mechanical parameters. The Bonferroni comparison was used for pairwise comparisons. The receiver operating characteristic curve (ROC) analysis and area under the ROC curve (AUROC) were calculated to evaluate the accuracy of the test. Sensitivity, specificity, and 95% CI were determined by the estimated optimal cut-off, using the Youden index. The Mann–Whitney *U*-test was used to compare the DR and G″ by fibrosis grade and was used to compare demographics, clinical characteristics, and imaging parameters related to DR and G″ as continuous variables. Fisher's exact test was applied for categorical parameters. The Jonckheere–Terpstra test was used to analyze the trend between histological data and parameters obtained by 3D MRE.

Statistical significance was defined as $p < 0.05$. Statistical analyses were performed with EZR (Saitama Medical Center, Jichi Medical University), which is a graphical user interface for R (the R Foundation for Statistical Computing).

RESULTS

Characteristics of the 39 patients

The background characteristics of patients in this study are shown in Table 1. Regarding fibrosis, six (15.4%), six (15.4%), nine (23.1%), 14 (35.9%), and four (10.3%) patients were diagnosed as F0, F1, F2, F3, and F4, respectively. As for variables related to inflammation, lobular inflammation 0, 1, and 2 were found in seven (17.9), 23 (59.0), and nine (23.1), and ballooning 0, 1, and 2 were found in nine (23.1), 23 (59.0), and seven (17.9) of those patients. Steatosis 1, 2, and 3 were observed in 22 (56.4), 10 (25.6), and seven (17.9), respectively.

Association of histological fibrosis, histological inflammation, and histological steatosis

We first investigated the association between histological fibrosis and histological hepatitis activity in the 39 patients, as well as the association between histological fibrosis and histological steatosis (Figure 2). As shown in Figure 2a, the activity score gradually increases with the advancement of fibrosis and all patients with F3 or higher had active hepatitis of A1 or higher. However, hepatitis activity may not be seen in some of the liver tissues in the early stages of disease, between F0 and F2 fibrosis.

Figure 2b shows the relationship between histological fibrosis and histological steatosis; all patients with any stage of fibrosis had histological steatosis of S1 or more. However, severe steatosis tended to be observed in the early stages of fibrosis.

Relationship between liver biopsy findings and parameters obtained by 3D MR elastography

Figure 3 shows the relationship between histological fibrosis and the parameters obtained by MRE. The association between shear stiffness and histological fibrosis is shown in Figure 3a; shear stiffness increases significantly as the F stage progresses. On the other hand, as shown in Figure 3b, PDFF values were not affected by the progression of fibrosis from F0 to F3, but tended to decrease with progression to F4. Figure 3c shows the relationship between the DR and histological fibrosis, indicating that the DR had a trend to increase from F0 to F2, but changed to a decreasing trend after F3. G'' increases as the F stage progresses, as shown in Figure 3d.

Association of damping ratio and loss modulus (G'') with histological activity

Figure 4 shows the relationship between histological activity and DR and G''. Because previous studies have reported that the DR is associated with hepatitis activity during the early stages of fibrosis and that the DR no longer reflects hepatitis activity as liver fibrosis progresses, we analyzed the associations between activity and DR in two ways: in all patients and in the patients with early fibrosis. Figure 4a shows the relationship between DR and hepatitis activity in all patients, while the relationship between G'' and hepatitis activity is shown in Figure 4b. The association between DR and activity was not significant ($p = 0.14$), and DR was not associated with ballooning ($p = 0.19$) or intralobular inflammation ($p = 0.18$), the two components of activity (Figure 4a). On the other hand, G'' was significantly

associated with activity ($p < 0.01$), ballooning ($p < 0.01$), and lobular inflammation ($p < 0.01$) (Figure 4b).

Figure 5 shows the analysis limited to patients with mild fibrosis up to F2. Hepatitis activity was significantly associated with DR, and DR increased as hepatitis activity increased ($p = 0.02$) (Figure 5a). When we examined the association of DR with ballooning and lobular inflammation, which are components of hepatitis activity, ballooning was significantly associated with DR ($p < 0.01$), but the association was not evident for lobular inflammation ($p = 0.20$). G″ was significantly associated with hepatitis activity ($p = 0.03$), and ballooning ($p = 0.04$), but the association was not significant for lobular inflammation ($p = 0.06$) (Figure 5b).

We also examined the association of DR and G″ with hepatitis activity in patients with advanced fibrosis stages F3 and F4. DR was significantly associated with lobular inflammation ($p = 0.02$), but not with hepatitis activity or ballooning. G″ was not significantly associated with hepatitis activity, ballooning, or lobular inflammation (Figure S1).

The optimal DR cutoff value associated with the appearance of hepatitis activity in patients with up to the F2 stage by ROC analysis was 0.094, with an AUC of 0.775, sensitivity of 81.2% and specificity of 80.0%, whereas the G″ cutoff value was 0.402, with an AUC of 0.825, sensitivity of 87.5%, and specificity of 80.0% (Figure S2).

Association of damping ratio and loss modulus (G″) with histological steatosis

Figure S3 shows the association of DR and G″ with histological steatosis. Here, we also investigated the relationship in two ways, i.e., in all patients (Figure S3a1,b1) and in patients with up to stage F2 fibrosis (Figure S3a2,b2), and found no evident association between histological steatosis and the DR or G″ in either analysis.

Clinical variables in those with high- and low-damping ratio and G″ values among patients within the F2 stage

We next divided patients within F0–2 stage fibrosis into two groups according to the DR cutoff value 0.094 and investigated the clinical factors showing an association with DR values. As shown in Table 2, the patients with DR ≥0.094 showed statistically significance in high ferritin ($p = 0.02$). On the other hand, as shown in Table 3, patients with G″ ≥0.402 showed statistical significance in high BMI ($p = 0.02$), high FIB-4 ($p < 0.01$), low platelets ($p < 0.01$), high prothrombin time-international normalized ratio ($p = 0.02$), high shear stiffness ($p < 0.01$), and high fibrosis stage ($p = 0.03$).

DISCUSSION

In this study, we investigated the relationship between liver histology and the parameters obtained through 3D-MRE analysis in Japanese patients with NAFLD, with a particular focus on detecting histological activity, and found that the DR and the loss modulus (G″) significantly correlated with the histological activity in the early stage of disease, as has been reported for White patients with NAFLD.[15,16,21] We also found that histological ballooning,

one of the factors constituting histological activity, was also significantly correlated with the DR and the G″.

While the clinical usefulness of MRI has been established in the evaluation of fibrosis by MRE and fat deposition by MRI-PDFF, the evaluation of inflammation by MRI has been difficult. Only recently, the viscosity index DR or G″, one of the parameters obtained by 3D-MRE, was found to reflect inflammation in the early stages of liver disease in several inflammation-induced mouse models, such as CCl4 and ARPKD mice, and even in human patients with NAFLD. On the other hand, it cannot be ruled out that a difference in ethnic background might affect the clinical course of NAFLD, as those patients included in previous studies were White. In our study, we confirmed that the relationship between inflammation and the DR and the G″ may be observed in Japanese patients. The results indicate that the DR and the G″ are useful in the diagnosis of early inflammation in both White and Japanese people, suggesting that the role of the DR and the G″ in the diagnosis of early inflammation may be universal. We consider this finding may lead physicians to intervene more aggressively in the management of early-stage NASH (e.g., calorie-restricted diets and moderate-intensity exercise). On the other hand, the large number of patients with fatty liver makes it difficult to perform 3D MRE on all patients with NAFLD. In this study, clinical parameters related to G″ and DR values included ferritin, FIB-4 index, and platelet levels. Therefore, patients with abnormalities in these parameters are considered candidates for DR and G″ measurements. However, in terms of clinical application, further study on narrowing down the target population is needed.

What is the underlying mechanism through which the DR and the G″ reflects inflammation? In liver diseases or conditions other than NAFLD/NASH, the DR was also reported to reflect portal hypertension,[23] inflammation in viral hepatitis, or biliary tract obstruction. The DR was also reported as an indicator of brain damage induced by certain diseases and its value was associated with memory loss.[30] In those previous studies using 3D MRI-related parameters, both stiffness and DR were used as a set to evaluate the histological conditions of each disease. In the CCl4 mouse model, the DR increased when the edema of liver tissue became pronounced and decreased with the appearance of fibrosis and, in the ARPKD mouse model, the DR increased in the early stages of liver injury, even before the appearance of inflammatory cell infiltration. In the elastic component of a tissue, the stored energy (shear stiffness [G*], storage modulus [G′]) is contributed primarily by solid elements such as fibers and cytoskeleton, while the energy dissipated by the viscous component (DR, G″) is a function of the liquid domain such as edema and blood perfusion.

In our study, the DR was associated with hepatocyte ballooning rather than inflammatory cell infiltration in the liver, suggesting that inflammation-related cell swelling may be one of the parameters that increase the DR. Although the pathomorphological background of “ballooning” in NASH is not completely understood, it is considered to occur because of fat deposition in hepatocytes, resulting in unstable cell morphology and endoplasmic reticulum enlargement, and thus leading to cell swelling.[31,32] In ballooning hepatocytes, the cytoskeletal system may be damaged by the reduction of keratins 8/18.[32] Although the present results indicate that inflammation-induced ballooning of hepatocytes is involved in DR and G″ changes, the correlation with hepatic inflammation becomes obscured and lost

when fibrosis becomes apparent. This is thought to be due to the complex involvement of pathological conditions such as portal hypertension and bile stasis, in addition to edema associated with inflammation, as fibrosis progresses. Therefore, DR and G″ is particularly useful to detect hepatic inflammation before the evident appearance of advanced fibrosis. The reason for the lack of association with lobular inflammation may involve the process of inflammation. Vasodilation, increased blood flow, increased vascular permeability, and interstitial fluid extravasation precede inflammatory cell infiltration into the interstitium.[33] It has been suggested that G″ may be elevated even before the presence of histological inflammation of cellular invasion,[34] which may be one reason for the lack of association between G″ or DR and histologically detectable lobular inflammation. Logically, the role of G″ and DR to detect activity might be slightly different. In the complete absence of fibrosis, G″ might be keener to detect activity while DR, corrected by the G′, might reflect activity more accurately than G″ in the appearance of mild fibrosis by avoiding the influence of fibrosis, although further studies are needed.

In this study, we also examined the association between liver steatosis and the DR and the G″ in patients with NAFLD, and found no clear association between liver steatosis in liver tissue and the DR and the G″. As there is no clear association between liver steatosis and DR, G″ has been reported in the NASH mouse model during the early stage, our results are also consistent with those previous findings, suggesting that fat deposition in hepatocytes in the early stage has little effect on the viscosity of the liver. However, we consider that this result does not indicate a direct relationship between fat deposition and the DR and G″, but may reflect inflammation rather than fat itself, because fat deposition decreases during the late stage of hepatitis as “burn-out” NASH, indicating the opposed dynamics of inflammation and fat deposition with diminished viable hepatocytes.

Our study has several limitations. First, the data obtained in our study were at a single frequency (60 Hz); DR and G″ are known to be frequency dependent, with lower frequencies reflecting inflammation activity more. Second, the slice thickness was large (5 mm) and the number of slices acquired were small (seven slices). This setting results in low *z*-axis resolution, so optimization of the conditions is necessary. Third, the study included seven HCC cases. Although 3D MRE measurements were performed at non-HCC sites and at HCC sites, the influence of HCC complications on the values of G″ and DR cannot be completely ruled out.

The usefulness of DR and G″ values in the initial diagnosis of inflammation has been confirmed by previous studies, as well as the current one. However, there is no clear information from previous studies on the effects of DR and “G” values on long-term prognosis, and we do not have clear data yet. In other words, future studies will be necessary to determine the dynamics of DR and G″ values in the clinical course of individual patients and their involvement in the long-term progression of fibrosis, as well as whether DR and G″ values can be used as markers reflecting the effects of therapeutic interventions, such as exercise, diet, and therapeutic drugs.

In conclusion, this study demonstrates that the DR and G″ obtained by 3D-MRE is an important biomarker for the appearance of inflammation in Japanese patients with early

NAFLD, indicating that 3D-MRE is a powerful noninvasive tool to disclose hepatic change in fibrosis, fat deposition, and inflammation, which was previously only obtained by the histological analysis of liver tissue.

Supplementary Material

Refer to Web version on PubMed Central for supplementary material.

ACKNOWLEDGMENTS

We thank Richard L. Ehman (Mayo Clinic) for providing the equipment of 3D MRE technology used in this study (supported by NIH R37 EB001981) and GE Healthcare technical support. This study was partly supported by the Research Program on Hepatitis of the Japanese Agency for Medical Research and Development (AMED) Japan (grant numbers 21fk0210072s0602, 21fk0210065s0602, 21fk0210 058s0703, and 21fk0210047h0003).

Funding information

Japan Agency for Medical Research and Development, Grant/Award Numbers: 21fk0210047h0003, 21fk0210058s0703, 21fk0210065s0602, 21fk0210072s0602

Abbreviations:

DR	damping ratio
HCC	hepatocellular carcinoma
MRE	MR elastography
NAFLD	nonalcoholic fatty liver disease
NASH	nonalcoholic steatohepatitis

REFERENCES

1. Younossi ZM, Koenig AB, Abdelatif D, Fazel Y, Henry L, Wymer M. Global epidemiology of nonalcoholic fatty liver disease-meta-analytic assessment of prevalence, incidence, and outcomes. Hepatology 2016;64(1):73–84. 10.1002/hep.28431 [PubMed: 26707365]
2. Ito T, Ishigami M, Zou B, Tanaka T, Takahashi H, Kurosaki M, et al. The epidemiology of NAFLD and lean NAFLD in Japan: a meta-analysis with individual and forecasting analysis, 1995–2040. Hepatol Int 2021;15(2):366–79. 10.1007/s12072-021-10143-4 [PubMed: 33580453]
3. Hamaguchi M, Kojima T, Takeda N, Nakagawa T, Taniguchi H, Fujii K, et al. The metabolic syndrome as a predictor of nonalcoholic fatty liver disease. Ann Intern Med 2005;143(10):722–8. 10.7326/0003-4819-143-10-200511150-00009 [PubMed: 16287793]
4. Estes C, Anstee QM, Arias-Loste MT, Bantel H, Bellentani S, Caballeria J, et al. Modeling NAFLD disease burden in China, France, Germany, Italy, Japan, Spain, United Kingdom, and United States for the period 2016–2030. J Hepatol 2018;69(4):896–904. 10.1016/j.jhep.2018.05.036 [PubMed: 29886156]
5. Ascha MS, Hanouneh IA, Lopez R, Tamimi TA, Feldstein AF, Zein NN. The incidence and risk factors of hepatocellular carcinoma in patients with nonalcoholic steatohepatitis. Hepatology 2010;51(6): 1972–8. 10.1002/hep.23527 [PubMed: 20209604]
6. Dyson J, Jaques B, Chattopadyhay D, Lochan R, Graham J, Das D, et al. Hepatocellular cancer: the impact of obesity, type 2 diabetes and a multidisciplinary team. J Hepatol 2014;60(1):110–7. 10.1016/j.jhep.2013.08.011 [PubMed: 23978719]

7. Hashimoto E, Yatsuji S, Tobari M, Taniai M, Torii N, Tokushige K, et al. Hepatocellular carcinoma in patients with nonalcoholic steatohepatitis. J Gastroenterol 2009;44(Suppl 19):89–95. 10.1007/s00535-008-2262-x [PubMed: 19148800]
8. Kawamura Y, Arase Y, Ikeda K, Seko Y, Imai N, Hosaka T, et al. Large-scale long-term follow-up study of Japanese patients with non-alcoholic fatty liver disease for the onset of hepatocellular carcinoma. Am J Gastroenterol 2012;107(2):253–61. 10.1038/ajg.2011.327 [PubMed: 22008893]
9. Chalasani N, Younossi Z, Lavine JE, Charlton M, Cusi K, Rinella M, et al. The diagnosis and management of nonalcoholic fatty liver disease: practice guidance from the American Association for the Study of Liver Diseases. Hepatology 2018;67(1):328–57. 10.1002/hep.29367 [PubMed: 28714183]
10. Jang SY, Tak WY, Park SY, Kweon YO, Lee YR, Kim G, et al. Diagnostic efficacy of serum Mac-2 binding protein glycosylation isomer and other markers for liver fibrosis in non-alcoholic fatty liver diseases. Ann Lab Med 2021;41(3):302–9. 10.3343/alm.2021.41.3.302 [PubMed: 33303715]
11. Andersson A, Kelly M, Imajo K, Nakajima A, Fallowfield JA, Hirschfield G, et al. Clinical utility of MRI biomarkers for identifying NASH patients at high risk of progression: a multicenter pooled data and meta-analysis. Clin Gastroenterol Hepatol 2021;20(11):2451–61. e3. 10.1016/j.cgh.2021.09.041 [PubMed: 34626833]
12. Hoodeshenas S, Yin M, Venkatesh SK. Magnetic resonance elastography of liver: current update. Top Magn Reson Imag 2018;27(5): 319–33. 10.1097/rmr.0000000000000177
13. Wilder J, Patel K. The clinical utility of FibroScan(®) as a noninvasive diagnostic test for liver disease. Med Devices (Auckl) 2014;7: 107–14. 10.2147/mder.s46943 [PubMed: 24833926]
14. Yin M, Talwalkar JA, Glaser KJ, Manduca A, Grimm RC, Rossman PJ, et al. Assessment of hepatic fibrosis with magnetic resonance elastography. Clin Gastroenterol Hepatol 2007;5(10):1207–13.e2. 10.1016/j.cgh.2007.06.012 [PubMed: 17916548]
15. Allen AM, Shah VH, Therneau TM, Venkatesh SK, Mounajjed T, Larson JJ, et al. Multiparametric magnetic resonance elastography improves the detection of NASH regression following bariatric surgery. Hepatol Commun 2020;4(2):185–92. 10.1002/hep4.1446 [PubMed: 32025604]
16. Allen AM, Shah VH, Therneau TM, Venkatesh SK, Mounajjed T, Larson JJ, et al. The role of three-dimensional magnetic resonance elastography in the diagnosis of nonalcoholic steatohepatitis in obese patients undergoing bariatric surgery. Hepatology 2020; 71(2):510–21. 10.1002/hep.30483 [PubMed: 30582669]
17. Garteiser P, Pagé G, d'Assignies G, Leitao HS, Vilgrain V, Sinkus R, et al. Necro-inflammatory activity grading in chronic viral hepatitis with three-dimensional multifrequency MR elastography. Sci Rep 2021;11(1):19386. 10.1038/s41598-021-98726-x [PubMed: 34588519]
18. Leitão HS, Doblas S, Garteiser P, d'Assignies G, Paradis V, Mouri F, et al. Hepatic fibrosis, inflammation, and steatosis: influence on the MR viscoelastic and diffusion parameters in patients with chronic liver disease. Radiology 2017;283(1):98–107. 10.1148/radiol.2016151570 [PubMed: 27788034]
19. Li J, Liu H, Mauer AS, Lucien F, Raiter A, Bandla H, et al. Characterization of cellular sources and circulating levels of extracellular vesicles in a dietary murine model of nonalcoholic steatohepatitis. Hepatol Commun 2019;3(9):1235–49. 10.1002/hep4.1404 [PubMed: 31497744]
20. Ma Y, Wang G, Gao F, Ma B, Song Q, Zhong S, et al. Clinical utility of 3D magnetic resonance elastography in patients with biliary obstruction. Eur Radiol 2022;32(3):2050–9. 10.1007/s00330-021-08295-w [PubMed: 34791513]
21. Qu Y, Middleton MS, Loomba R, Glaser KJ, Chen J, Hooker JC, et al. Magnetic resonance elastography biomarkers for detection of histologic alterations in nonalcoholic fatty liver disease in the absence of fibrosis. Eur Radiol 2021;31(11):8408–19. 10.1007/s00330-021-07988-6 [PubMed: 33899143]
22. Shi Y, Qi YF, Lan GY, Wu Q, Ma B, Zhang XY, et al. Three-dimensional MR elastography depicts liver inflammation, fibrosis, and portal hypertension in chronic hepatitis B or C. Radiology 2021;301(1):154–62. 10.1148/radiol.2021202804 [PubMed: 34374594]
23. Yin M, Glaser KJ, Manduca A, Mounajjed T, Malhi H, Simonetto DA, et al. Distinguishing between hepatic inflammation and fibrosis with MR elastography. Radiology 2017;284(3):694–705. 10.1148/radiol.2017160622 [PubMed: 28128707]

24. Yin Z, Murphy MC, Li J, Glaser KJ, Mauer AS, Mounajjed T, et al. Prediction of nonalcoholic fatty liver disease (NAFLD) activity score (NAS) with multiparametric hepatic magnetic resonance imaging and elastography. Eur Radiol 2019;29(11):5823–31. 10.1007/s00330-019-06076-0 [PubMed: 30887196]
25. Wong RJ, Ahmed A. Obesity and non-alcoholic fatty liver disease: disparate associations among Asian populations. World J Hepatol 2014;6(5):263. 10.4254/wjh.v6.i5.263 [PubMed: 24868320]
26. Bambha K, Belt P, Abraham M, Wilson LA, Pabst M, Ferrell L, et al. Ethnicity and nonalcoholic fatty liver disease. Hepatology 2012; 55(3):769–80. 10.1002/hep.24726 [PubMed: 21987488]
27. Bonacini M, Kassamali F, Kari S, Lopez Barrera N, Kohla M. Racial differences in prevalence and severity of non-alcoholic fatty liver disease. World J Hepatol 2021;13(7):763–73. 10.4254/wjh.v13.i7.763 [PubMed: 34367497]
28. Bugianesi E, Bugianesi E, eds. NASH in lean individuals. Semin Liver Dis 2019;39(1):86–95. 10.1055/s-0038-1677517 [PubMed: 30654392]
29. Hsu C, Caussy C, Imajo K, Chen J, Singh S, Kaulback K, et al. Magnetic resonance vs transient elastography analysis of patients with nonalcoholic fatty liver disease: a systematic review and pooled analysis of individual participants. Clin Gastroenterol Hepatol 2019;17(4):630–7.e8. 10.1016/j.cgh.2018.05.059 [PubMed: 29908362]
30. Murphy MC, Huston J III, Ehman RL. MR elastography of the brain and its application in neurological diseases. Neuroimage 2019;187: 176–83. 10.1016/j.neuroimage.2017.10.008 [PubMed: 28993232]
31. Caldwell S, Ikura Y, Dias D, Isomoto K, Yabu A, Moskaluk C, et al. Hepatocellular ballooning in NASH. J Hepatol 2010;53(4):719–23. 10.1016/j.jhep.2010.04.031 [PubMed: 20624660]
32. Tannapfel A, Denk H, Dienes HP, Langner C, Schirmacher P, Trauner M, et al. Histopathological diagnosis of non-alcoholic and alcoholic fatty liver disease. Virchows Arch 2011;458(5):511–23. 10.1007/s00428-011-1066-1 [PubMed: 21442288]
33. Kumar V, Abbas AK, Aster JC, Perkins JA, Robbins SL. Robbins basic pathology 10th ed. Elsevier; 2018;xiv:935. https://ci.nii.ac.jp/ncid/BB23428711
34. Li J, Allen AM, Shah VH, Manduca A, Ehman RL, Yin M. Longitudinal changes in MR elastography-based biomarkers in obese patients treated with bariatric surgery. Clin Gastroenterol Hepatol 2021; S1542-3565(21)01146-0. 10.1016/j.cgh.2021.10.033

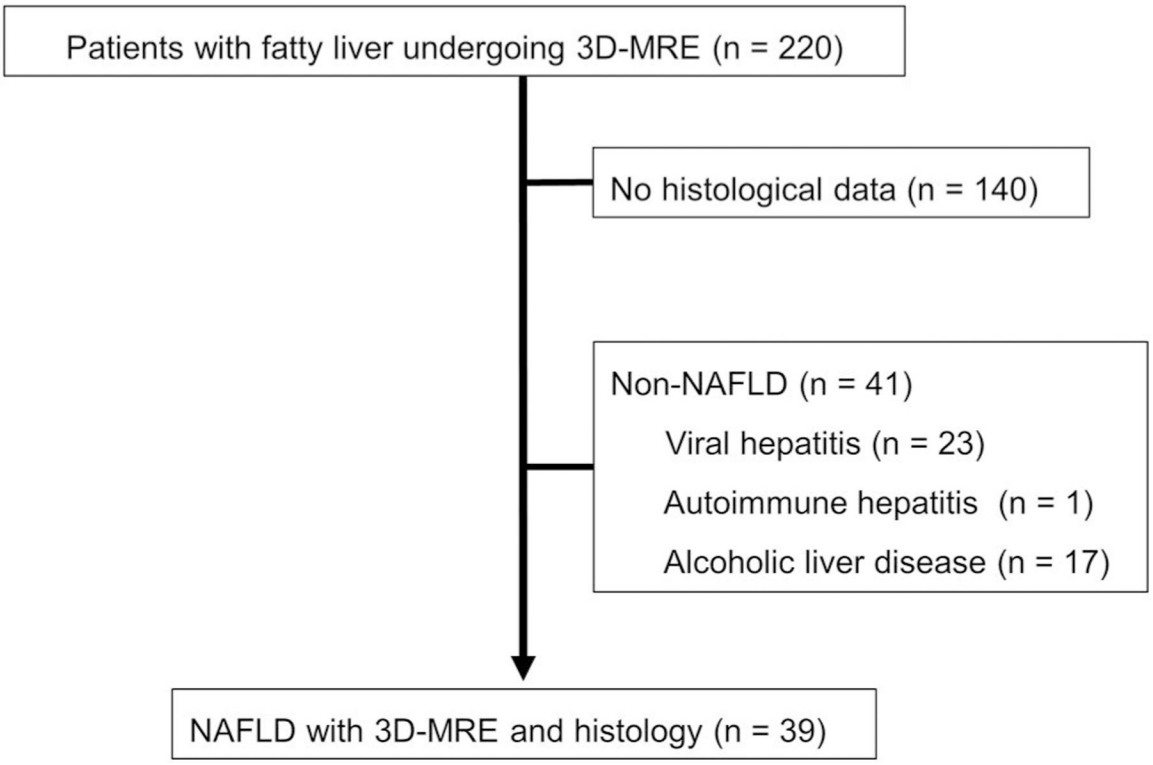

FIGURE 1.
Flow chart for the inclusion of patients in this study. 3D MRE, magnetic resonance elastography; NAFLD, nonalcoholic fatty liver disease

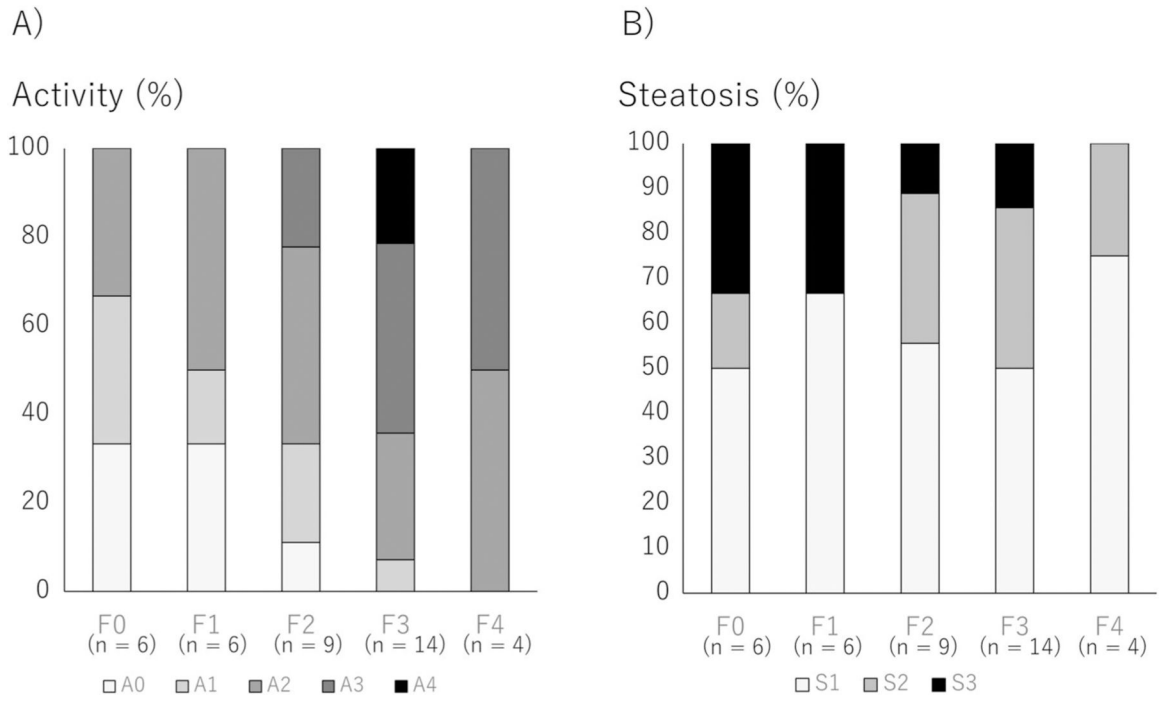

FIGURE 2.

Association of histological fibrosis, histological inflammation, and histological steatosis. Association between histological fibrosis and histological hepatitis activity and the association between histological fibrosis and histological steatosis were investigated. (a) Association between histological fibrosis and histological inflammation. (b) Association between histological fibrosis and histological steatosis.

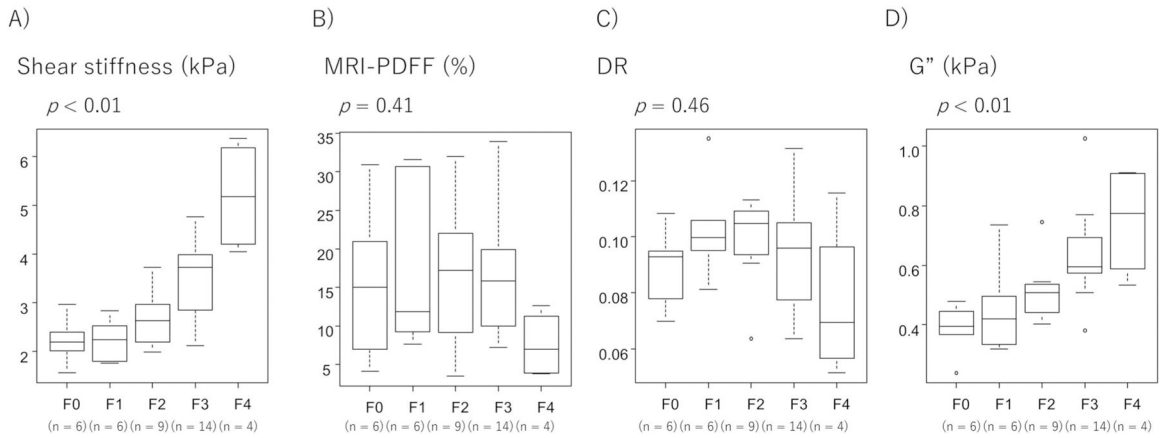

FIGURE 3.

Relationship between liver biopsy findings and parameters obtained by 3D MRE. (a) Association between histological fibrosis and 3D MRE-derived shear stiffness. (b) Association between histological fibrosis and 3D MRE-derived PDFF. (c) Association between histological fibrosis and 3D MRE-derived DR. (d) Association between histological fibrosis and loss modulus (G″). DR, damping ratio; 3D MRE, magnetic resonance elastography; PDFF, proton density fat fraction

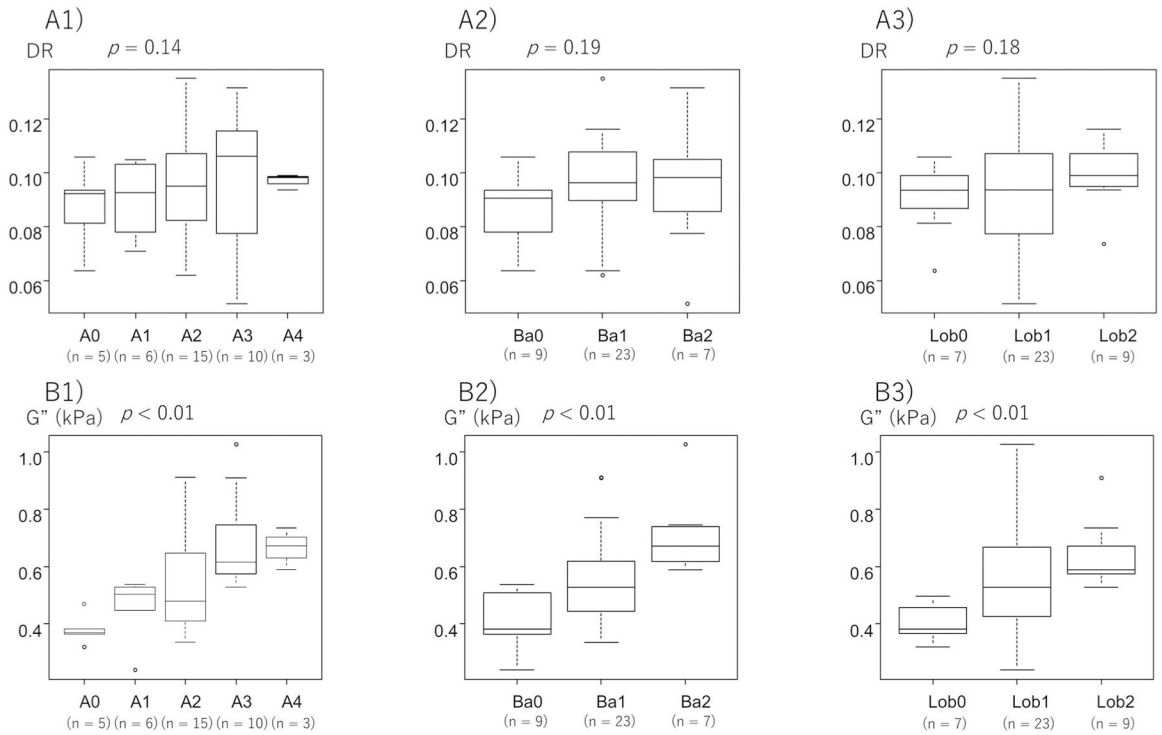

FIGURE 4.

Association of DR and loss modulus (G″) with histological activity. Relationship between the DR and (a1) histological activity, (a2) ballooning, and (a3) lobular inflammation in patients with all stages of fibrosis. Relationship between G″ and (b1) histological activity, (b2) ballooning, and (b3) lobular inflammation in patients. DR, damping ratio

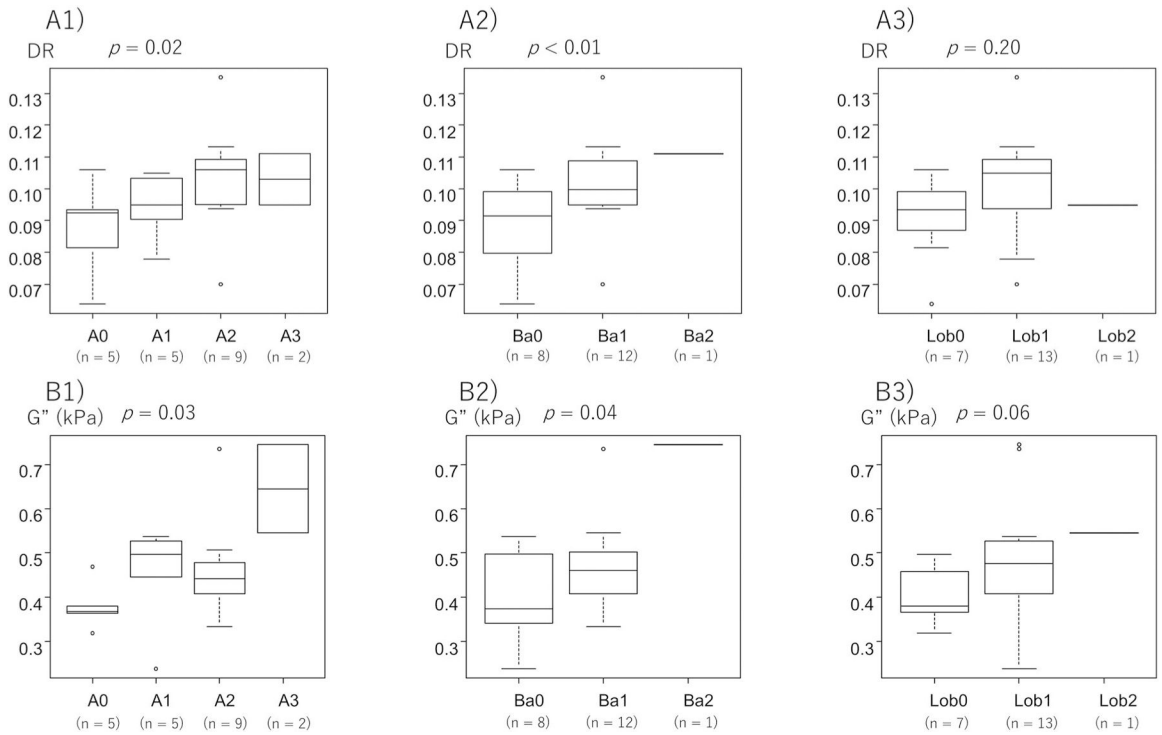

FIGURE 5.

Association of DR and loss modulus (G″) with histological activity with up to stage F2 fibrosis. Relationship between the DR and (a1) histological activity, (a2) ballooning, and (a3) lobular inflammation in patients with all stages of fibrosis with up to stage F2 fibrosis. Relationship between the G″ and (b1) histological activity, (b2) ballooning, and (b3) lobular inflammation in patients. DR, damping ratio

TABLE 1

Baseline demographic characteristics of the participants

Variable		***N* = 39**
Sex, male		21 (53.8)
Age (years)		63.00 [49.50–68.50]
BMI (kg/m^2)		27.37 [24.86–30.39]
Diabetes		19 (48.7)
Hypertension		17 (43.6)
Dyslipidemia		24 (61.5)
Biochemical data		
Albumin (g/dl)		4.4 [4.3–4.6]
Total bilirubin (mg/dl)		0.8 [0.6–0.9]
Alkaline phosphatase (U/L)		247 [199–320]
γ-GTP (U/L)		70 [37–100]
AST (U/L)		55 [44–69]
ALT (U/L)		64 [46–100]
Platelets (10^3/mm^3)		192 [161–227]
PT-INR		1.04 [0.97–1.06]
FIB-4 index		2.01 [1.53–2.64]
Histological data		
Steatosis (%)	1/2/3	22 (56.4)/10 (25.6)/7 (17.9)
Lobular inflammation (%)	0/1/2	7 (17.9)/23 (59.0)/9 (23.1)
Ballooning (%)	0/1/2	9 (23.1)/23 (59.0)/7 (17.9)
NAS score (%)		3 [3–5]
Fibrosis stage (%)	0/1/2/3/4	6 (15.4)/6 (15.4)/9 (23.1)/14 (35.9)/4 (10.3)
MRI parameter		
PDFF (%)		13.1 [9.0–20.9]
G″ LM (kPa)		0.53 [0.43–0.64]
G′ SM (kPa)		2.75 [2.17–3.76]
SS (kPa)		2.85 [2.23–3.84]
DR		0.09 [0.08–0.11]

Note: Data are expressed as *n* (%) or median [IQR].

Abbreviations: BMI, body mass index; DR, damping ratio; FIB-4, Fibrosis-4 index; γ-GTP, gamma-glutamyl transpeptidase; LM, loss modulus; MRI, magnetic resonance imaging; NAS, nonalcoholic fatty liver disease activity score; PDFF, proton density fat fraction; PT-INR, prothrombin time-international normalized ratio; SM, storage modulus; SS, shear stiffness.

TABLE 2

Characteristics of clinical variables in those with high- and low-DR values among patients with F0–2

	DR <0.094	**DR ≥0.094**	
	***n* = 8**	***n* = 13**	***p*-value**
Sex, male	5 (62)	10 (76)	0.63
Age (years)	63 [48–67]	67 [49–71]	0.56
BMI (kg/m^2)	24.9 [24.1–27.0]	27.3 [24.1–31.4]	0.56
Albumin (g/dl)	4.7 [4.3–5.0]	4.5 [4.4–4.6]	0.33
Total bilirubin (mg/dl)	0.6 [0.4–0.9]	0.8 [0.7–1.1]	0.21
γ-GTP (U/L)	74 [30–85]	53 [30–70]	0.70
AST (U/L)	50 [35–62]	53 [39–72]	0.32
ALT (U/L)	65 [57–88]	70 [36–147]	0.73
FIB-4	1.64 [1.18–1.77]	1.67 [1.30–2.57]	0.49
Ferritin (ng/ml)	114 [97–175]	354 [187–508]	0.02
Platelets (10^3/mm^3)	217 [187–252]	194 [162–236]	0.49
PT-INR	0.98 [0.93–1.01]	0.98 [0.95–1.04]	0.73
M2BPGi	0.63 [0.48–1.06]	0.77 [0.64–0.82]	0.76
Type IV collagen 7s (ng/ml)	4.8 [4.0–5.5]	5.6 [4.8–6.3]	0.15
PDFF (%)	15.8 [11.8–20.6]	13.1 [7.8–22.0]	0.89
Alcohol (g/day)	0 [0–0]	5 [0–5]	0.08
SS (kPa)	2.15 [2.01–2.97]	2.40 [2.09–2.63]	0.94
Brunt stage	1 [0–2]	1 [1–2]	0.30

Note: Data are expressed as *n* (%) or median [IQR].

Abbreviations: BMI, body mass index; DR, damping ratio; FIB-4, Fibrosis-4 index; γ-GTP, gamma-glutamyl transpeptidase; PDFF, proton density fat fraction; PT-INR, prothrombin time-international normalized ratio; SS, shear stiffness.

TABLE 3

Characteristics of clinical variables in those with high- and low-G″ values among patients with F0–2

	G″ <0.402	**G″ ≥0.402**	
	***n* = 6**	***n* = 15**	***p*-value**
Sex, male	3 (50)	12 (80)	0.29
Age (years)	63 [52–66]	66 [48–71]	0.79
BMI (kg/m^2)	23.5 [23.3–24.6]	27.7 [25.2–32.7]	0.02
Albumin (g/dl)	4.6 [4.5–5.0]	4.4 [4.3–4.7]	0.34
Total bilirubin (mg/dl)	1.0 [0.6–1.2]	0.8 [0.6–0.9]	0.48
γ-GTP (U/L)	51 [30–82]	63 [32–81]	0.87
AST (U/L)	44 [20–60]	54 [39–66]	0.25
ALT (U/L)	80 [32–131]	63 [48–117]	0.90
FIB-4	1.06 [0.78–1.33]	1.91 [1.54–2.82]	0.01
Ferritin (ng/ml)	155 [114–219]	354 [143–494]	0.17
Platelets (10^3/mm^3)	259 [252–280]	188 [167–198]	0.01
PT-INR	0.92 [0.90–0.96]	1.00 [0.97–1.05]	0.02
M2BPGi	0.50 [0.44–0.64]	0.78 [0.70–0.92]	0.06
Type IV collagen 7s (ng/ml)	4.2 [4.0–5.0]	5.6 [5.0–6.4]	0.06
PDFF (%)	21.7 [10.0–30.8]	14.5 [8.4–20.9]	0.48
Alcohol (g/day)	0 [0–5]	5 [0–5]	0.58
SS (kPa)	1.90 [1.77–2.01]	2.53 [2.29–2.95]	0.01
Brunt stage	1 [0–1]	2 [0–2]	0.03

Note: Data are expressed as *n* (%) or median [IQR].

Abbreviations: BMI, body mass index; FIB-4, Fibrosis-4 index; γ-GTP, gamma-glutamyl transpeptidase; PDFF, proton density fat fraction; PT-INR, prothrombin time-international normalized ratio; SS, shear stiffness.